journal

J. Am. Ceram. Soc., 83 [9] 2189–95 (2000)

High-Temperature Flow Behavior of Ceramic Suspensions

T.-M. Gabriel Chu* and John W. Halloran*

Department of Materials Science and Engineering, University of Michigan, Ann Arbor, Michigan 48105

The objective of this study was to investigate the effects of temperature and solids loading on the viscosity of two nonaqueous ceramic suspensions. In this article, the viscosity of Al_2O_3 suspensions with 5%–50% solids loading and hydroxyapatite suspensions with a solids loading of 5%–40% were measured at temperatures of 25°, 45°, 65°, and 75°C. The high-shear Newtonian viscosity at various temperatures was reduced to a single curve by the reduced viscosity and the temperature-adjusted solids volume fraction of the suspensions. The Krieger–Dougherty model, with the intrinsic viscosity corrected for particle geometry, was fitted to the data and was observed to provide a satisfactory description to the solids-loading–viscosity data for both suspensions.

I. Introduction

TRADITIONALLY, ceramic slurries are processed at room temperature. Lately, processes for making complicated ceramic parts have been developed by jetting and printing ceramic slurries at elevated temperatures.[1–3] An understanding of the effect of solids loading on the viscosity of the suspensions at elevated temperatures is fundamental and essential in these processes. Theories on the effect of solids loading on the viscosity at room temperature have been developed by many researchers.[4–8] Many of these groups used idealized systems that contained monodispersed hard spherical particles and a one-component liquid medium to verify their theories. However, in practice, in ceramic processing, highly loaded ceramic suspensions deviate from the ideal system in several ways. The liquid medium usually contains more than one component, the ceramic particles are not always monodispersed, and dispersants usually are used to modify the interparticle force. Mathematical models on the solids-loading–viscosity relation of these "nonideal" ceramic suspensions are needed.

Relatively little literature was found regarding the temperature effect on the viscosity of highly loaded suspensions. Krieger[9] used the relative shear stress and the reduced viscosity to explain the temperature effect on Brownian force. Tsutsumi and Yoshida[10] used the product of the viscosity of the suspension medium and the shear rate to describe the effect of temperature on hydrodynamic force. An important factor in the high-temperature flow behavior of the highly loaded suspension is the effect of thermal expansion of the liquid medium. The flow behavior of a highly loaded suspension is known to be very sensitive to the variation in the solids loading.[4] One possible reason for a variation in solids loading is the temperature change in the suspensions. Because of the large difference in the coefficient of thermal expansion between solid and liquid, a change in the suspension temperature can have a strong effect on the solids loading, which, subsequently, would change the flow behavior. Although the effect of thermal expansion of the liquid phase has been mentioned,[11] no special treatment in this aspect has been noticed.

The first objective of this article is to study the effect of temperature on the viscosity of nonaqueous Al_2O_3 suspensions and hydroxyapatite (HA) suspensions. The intent is to correlate the viscosity to the temperature-adjusted solids loading of the ceramic suspensions at various temperatures. Generally, if a well-dispersed dilute ceramic suspension is prepared from a Newtonian fluid, the flow behavior of the suspension will remain Newtonian; the viscosity will be constant, regardless of the shear rate. However, in well-dispersed highly loaded suspensions, the viscosity of the suspension may or may not change with the shear rate, depending on the magnitude of the shear rate. In most cases, at extremely low shear rates, Brownian motion dominates and the structure of the particles in the suspension remains relatively undisturbed, despite the shearing. The viscosity in this region is independent of the shear rate and usually is called the "low-shear Newtonian limit" of the suspension. As the shear rate increases, the particle structure in the suspension is disrupted; the viscosity of the suspension decreases as the shear rate increases. This region usually is called the "shear-thinning region" of the flow curve. As the shear rate increases further, the particle structure in the suspension becomes grossly oriented; the viscosity of the suspension remains constant, irrespective of the shear rate. This region usually is called the "high-shear Newtonian limit" of the suspension.[4,12] For our research, we have focused on the high-shear Newtonian limit of the suspensions, because this region is most relevant to our processing condition.

The second objective of this study is to provide a mathematical description to the solids-loading–viscosity relation for these highly loaded ceramic suspensions. The Krieger–Dougherty model was applied to the solids-loading–viscosity data of both ceramic suspensions, where the solids packing factor and liquid intrinsic viscosity each were corrected for the particle shape. The usefulness of the model was evaluated.

II. Experimental Procedure

Al_2O_3 powder (Product A-16, Alcoa, Pittsburgh, PA) with an average size (d_{50}) of 0.4 μm was used in this study. The 90th percentile particle size (d_{90}) of this powder was 1.2 μm, and the 10th percentile particle size (d_{10}) was 0.14 μm (according to data from the manufacturer). Scanning electron microscopy (SEM) (Model S-800, Hitachi, Tokyo, Japan) indicated that the shape of the particles was approximately spherical. The density of the powder was 3.92 g/cm^3, and the specific surface area of this powder was 9.5 m^2/g (according to data from the manufacturer). The HA powder used was acicular, with a diameter of 60 nm and a length of 600 nm. The density of the powder was 3.14 g/cm^3, as measured via helium pycnometry (Model AccuPyc 1330, Micromeritics Instrument Corp., Norcross, GA.). The Brunauer–Emmett–Teller (BET) specific surface area of this powder was 17 m^2/g, as reported in the literature.[13]

The liquid medium was a 1:1 mixture of propoxylated neopentoglycol diacrylate (PNPGDA) and isobornyl acrylate (IBA). The dispersant used for the Al_2O_3 powder was a commercial product that was based on quaternary ammonium acetate (Emcol CC-55, Witco Corp., Houston, TX). First, the optimal dose of

V. A. Hackley—contributing editor

Manuscript No. 188998. Received October 22, 1999; approved March 14, 2000.
*Member, American Ceramic Society.

dispersant for the ceramic powder was determined. Al_2O_3 powder was dispersed in a PNPGDA/IBA premix to make a 20 vol% suspension. Six groups of suspensions, with dispersant doses of 0.5–3.5 wt% (dry powder weight), were prepared from the 20 vol% suspension. The viscosity of the suspension at different dispersant dosage levels was measured with a rheometer (Model CS-50, Bohlin, East Brunswick, NJ) in a cone-and-plate setting at shear rates of 1–1000 s^{-1}. The dispersant dose that yielded the lowest viscosity was used to prepare the Al_2O_3 suspensions in the rest of the experiments. The HA powder was dispersed with 5% (relative to the dry powder weight) of a 1:1 mixture of the propopoxy quaternary ammonium acetate and aromatic phosphate ester (Emphos CS-1361, Witco Corp.). The characterization and determination for the optimal dispersant dose for HA powder have been reported elsewhere.[14] With the optimal dispersant dose, a 50 vol% Al_2O_3 suspension and 40 vol% HA suspension were prepared by incrementally adding the ceramic powder to the PNPGDA/IBA premix along with the dispersant. Vigorous mixing was needed after each powder addition to disperse the powder.

Then, the 50 vol% Al_2O_3 suspension was diluted with the PNPGDA/IBA premix to make 5, 15, 30, 40, 42, 44, 46, 48, and 49 vol% suspensions. The viscosity of the suspensions at temperatures of 25°, 45°, 65°, and 75°C was measured using the previously mentioned Bohlin rheometer with a cone-and-plate geometry. The temperature was controlled by a heating plate on the cone-and-plate assembly and monitored by a thermocouple that was mounted in the lower plate. The gap size was set at 200 μm, and the steady shear viscosity was measured at each shear rate. The 40 vol% HA suspension also was diluted with the PNPGDA/IBA premix to make 5, 15, 30, 32, 34, 36, 38, and 39 vol% suspensions. The viscosity at 25°, 45°, 65°, and 75°C was measured as described previously. The viscosity of the PNPGDA/IBA premix without any ceramic fillers at these temperatures also was measured.

III. Results and Discussion

(1) High-Temperature Viscosity

In the PNPGDA/IBA premix, the viscosity was Newtonian at any given testing temperature. The viscosity of the premix decreased from 10 mPa·s to 4 mPa·s as the temperature increased from 25°C to 75°C. When the viscosity is plotted against the inverse of temperature, an Arrhenius relation is observed, as shown in Fig. 1. The calculated apparent activation energy was 17 kJ/mol. In the dispersant-dose study, the 20 vol% Al_2O_3/PNPGDA/IBA was pasty before any dispersant was added. The suspension started to flow with the addition of 0.52% of dispersant. The suspension viscosity gradually decreased as the dispersant dose was increased; the viscosity finally stabilized to ~40 mPa·s after a dispersant dose of 2%, as shown in Fig. 2. The excess amount of dispersants, in the range of 2%–3%, did not seem to have a significant effect on the viscosity of the 20 vol% Al_2O_3 suspension. A dispersant dose of 2% (or ~2 mg of dispersant per square meter of powder surface) was used to prepare the 50 vol% Al_2O_3 suspension. The dispersant dose for the HA suspension was 5%, relative to the dry powder weight (or ~3 mg dispersant per square meter of powder surface).

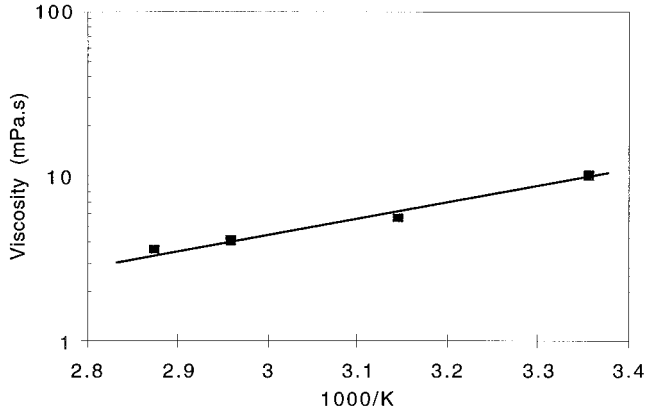

Fig. 1. Arrhenius plot of the monomer premix viscosity.

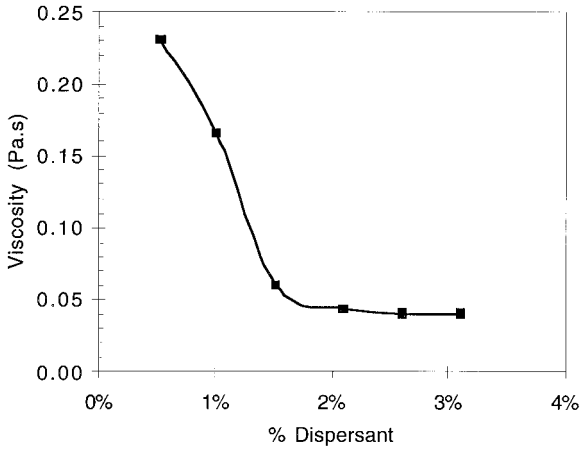

Fig. 2. Viscosity versus dispersant dose of 20 vol% Al_2O_3/PNPGDA/IBA. Al_2O_3 was dispersed with ammonium acetate, and the dispersant dose is the weight ratio of dispersant to Al_2O_3 dry powder. (Shear rate of 400 s^{-1}.)

The measured flow curves of both Al_2O_3 and HA suspensions, with various solids loadings at 25°C, are shown in Figs. 3 and 4, respectively. The Al_2O_3 suspensions and HA suspensions both were Newtonian at a solids loading of <15%. Shear-thinning regions appeared at a solids loading of ≥30%. Following the shear-thinning region, these suspensions approached a constant viscosity value: the high-shear Newtonian limit. As expected, the viscosity of the suspensions increased as the solids loading increased in both suspensions. The viscosity of the HA suspension was much higher, in comparison to the Al_2O_3 suspension. This result was not surprising, because the needle-shaped HA particles are less favorable hydrodynamically, in comparison to the spherical Al_2O_3 powders. The flow curves at 45°, 65°, and 75°C for both types of suspensions were similar to the 25°C data curves and are not shown here.

The effect of solids loading on the flow behavior at different temperatures was studied. The high-shear Newtonian viscosity of each suspension was determined from the high-shear Newtonian limit of the flow curves, where the viscosity stabilized to a constant value. Then, the high-shear Newtonian viscosity for the Al_2O_3 and HA suspensions were plotted against their respective solids loadings, as shown in Figs. 5 and 6, respectively. These curves have the typical shape of a plot of solids loading versus viscosity: low viscosity at low solids loadings and a sharp increase at high solids loadings. The viscosity of the suspensions was lower at higher testing temperatures. The high-shear Newtonian viscosity decreased in the 50% Al_2O_3 suspension when the temperature increased from 25°C to 75°C, from 0.95 Pa·s to 0.16 Pa·s (an 83% reduction). The high-shear Newtonian viscosity of the HA suspension also decreased, from 15.2 Pa·s to 2.2 Pa·s, which is an 86% reduction.

However, as the temperature increases, the monomer viscosity also decreases. To account for the change in suspension viscosity that resulted from the reduction in the monomer viscosity, a reduced viscosity was used instead of the apparent viscosity. The reduced viscosity was obtained by dividing the apparent viscosity of the suspension by the viscosity of the monomer at the same temperature. The other important factor is the thermal expansion of the liquid medium. As the temperature increases, the liquid medium undergoes considerably larger thermal expansion than the ceramics. The difference in the volume expansion between solid

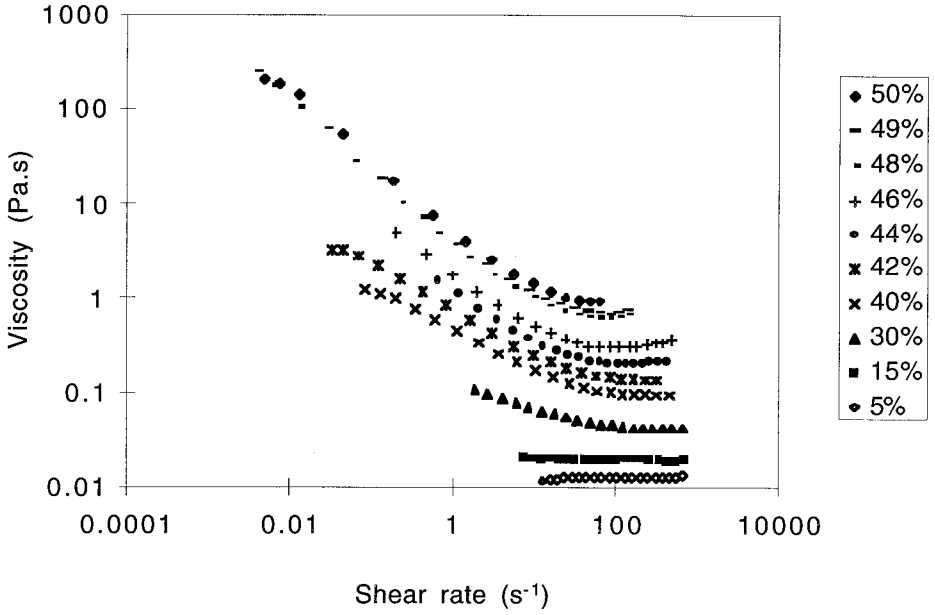

Fig. 3. Apparent viscosity of Al_2O_3/PNPGDA/IBA dispersed with 2% ammonium acetate at 25°C.

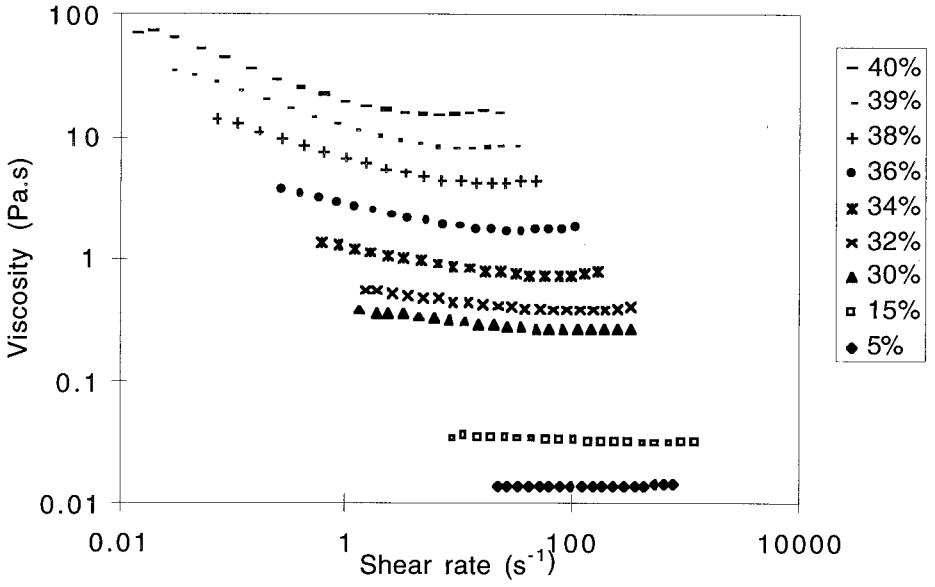

Fig. 4. Apparent viscosity of HA/PNPGDA/IBA dispersed with 5% ammonium acetate and phosphate ester at 25°C.

and liquid can change the solids loading in the suspension. The temperature-adjusted solids volume fraction ($\phi_{(temp)}$) can be expressed as follows:

$$\phi_{(temp)} = \frac{V_S + \Delta V_S}{(V_S + \Delta V_S) + (V_L + \Delta V_L)} \quad (1)$$

where V_S and V_L are the respective volume fractions of solid and liquid in the suspension, and ΔV_S and ΔV_L are the respective amounts of volume increase in the solid and liquid due to thermal expansion. The volumetric coefficient of thermal expansion of the liquid medium was measured to be 0.6×10^{-3} °C^{-1}. In Eq. (1), the amount of volume increase in ceramic powder due to thermal expansion (ΔV_S) is considerably small and can be ignored. Thus, the temperature-adjusted solids volume fraction becomes

$$\phi_{(temp)} = \frac{V_S}{V_S + V_L + \Delta V_L} \quad (2)$$

The temperature-adjusted solids fraction of suspensions at various temperatures was calculated with Eq. (2) and plotted against the corresponding reduced viscosity. The solids-loading–viscosity data were reduced to one curve for both Al_2O_3 and HA suspensions, as shown in Figs. 7 and 8, respectively.

Finally, the influence of Brownian rotation of the rod-shaped HA particles on the viscosity in the high-shear Newtonian region was evaluated at various temperatures. The rotary diffusivity for the rod-shaped HA particles can be calculated using the relation[15]

$$D = \frac{3kT\left[\ln\left(\frac{L}{d}\right) - 0.8\right]}{\pi\eta_0 L^3} \quad (3)$$

where D is the rotary diffusivity, k the Boltzmann's constant, T the absolute temperature, and η_0 the viscosity of the solvent; d and L represent the diameter and length of the rod, respectively. The Brownian influence on the suspension viscosity can be evaluated

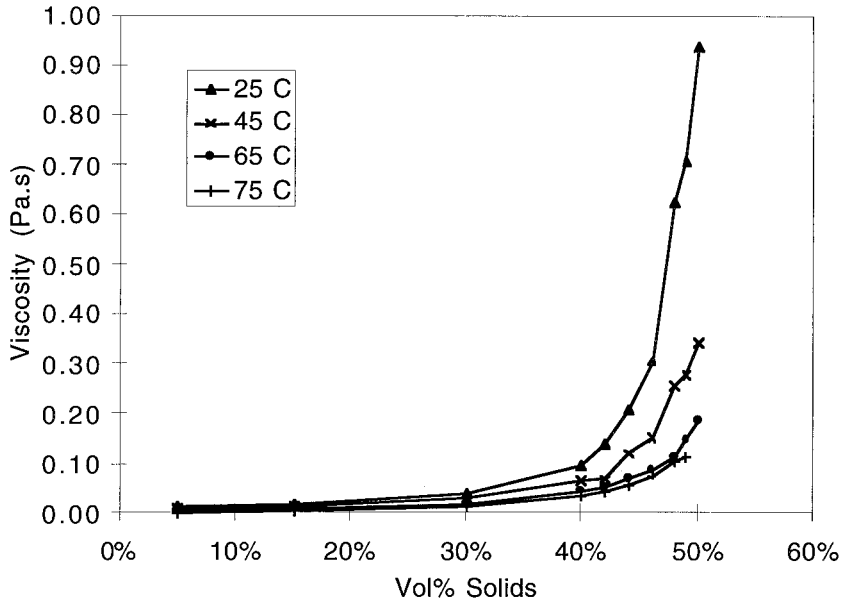

Fig. 5. Apparent viscosity of Al_2O_3/PNPGDA/IBA in the high-shear Newtonian region.

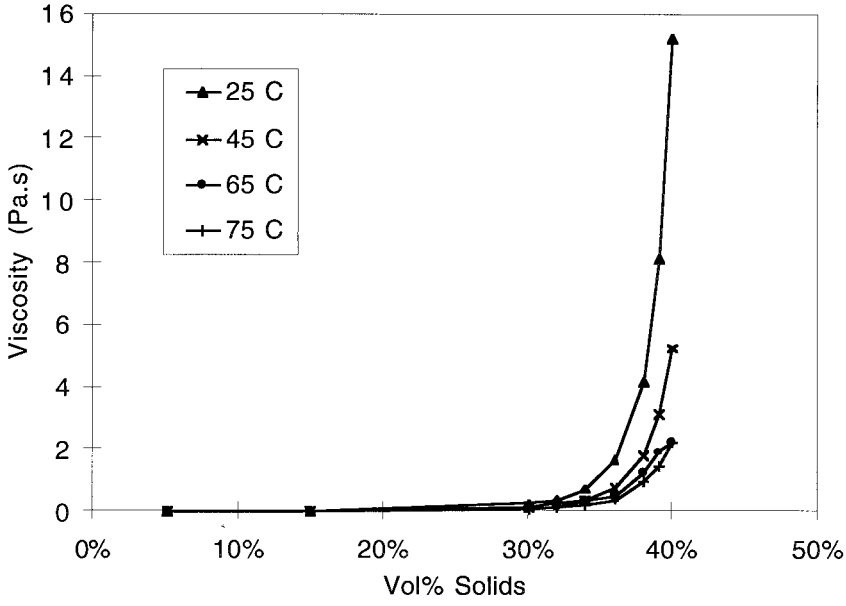

Fig. 6. Apparent viscosity of HA/PNPGDA/IBA in the high-shear Newtonian region.

by the rotational Peclet number (Pe):

$$\mathrm{Pe} \equiv \frac{\dot{\gamma}}{D} \tag{4}$$

Here, $\dot{\gamma}$ is the shear rate. At $\dot{\gamma} = 100\ s^{-1}$ and testing temperatures of 25°, 45°, 65°, and 75°C, the Pe value for the HA suspension was 30–40. Because $\mathrm{Pe} \gg 1$, HA particles can be considered to be non-Brownian.[15]

The results show that the reduced viscosity and the corrected solids fraction are useful scaling factors for reducing the high-temperature viscosity of highly loaded suspensions. The effect of solids loading on high-shear Newtonian viscosity at various temperatures can be explained by the reduction in monomer viscosity and the reduction in solids fraction in the suspension due to thermal expansion of the monomer.

It is recognized that dispersant adsorption in organic solvents can be temperature dependent and very complicated.[11] Variation in the temperature can influence the dispersant behavior in the solvent, which leads to changes in the interparticle interaction and, therefore, the floc structure of the suspension. This observation should be reflected in a shifting of the solids-loading–viscosity curve. The direction of shifting will be dependent on whether a formation or disruption of flocs has occurred from the change in interparticle interaction. In our results, all our high-temperature viscosity data were reduced to a single curve, which was indicative of the absence of significant floc formation or floc disruption. A possible reason for this observation is that the powder surface is completely covered by the dispersant at all times that these concentrated suspensions are fully dispersed; therefore, they have no significant floc structure. The exact mechanism for the complete dispersion is beyond the scope of this study. However, if the particles are, essentially, fully dispersed as singlets, the viscosity of the suspension can be modeled by the hydrodynamic interaction of well-dispersed particles. Thus, we expect our data to be described well by a hydrodynamic model such as the Krieger–Dougherty model.

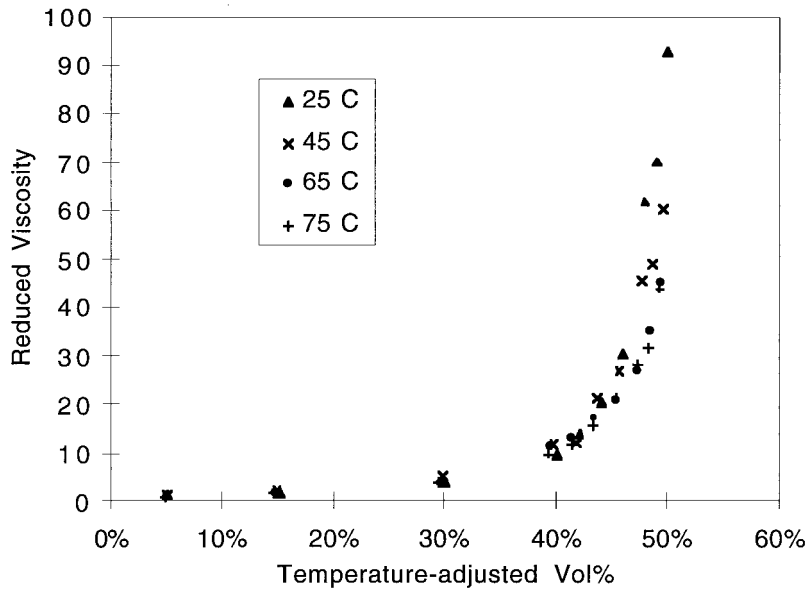

Fig. 7. Reduced viscosity of Al_2O_3/PNPGDA/IBA versus the temperature-adjusted solids loading.

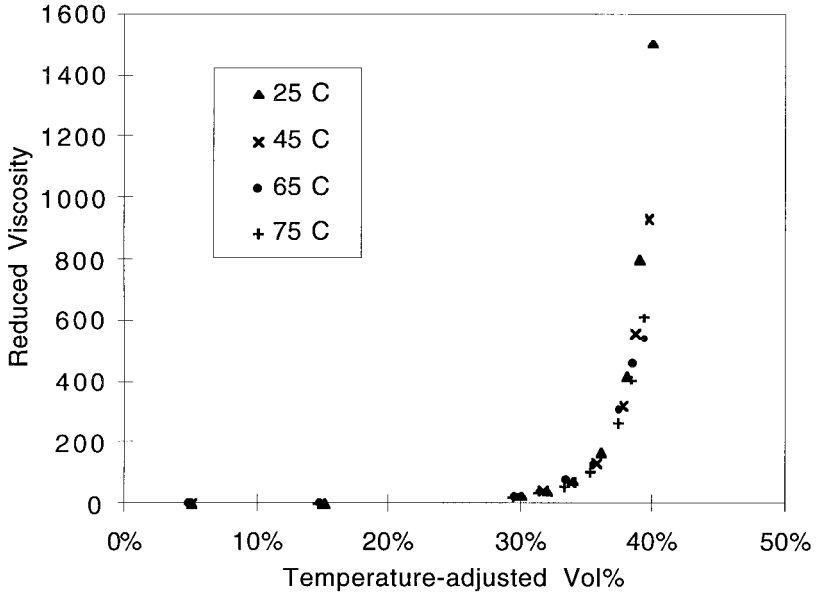

Fig. 8. Reduced viscosity of HA/PNPGDA/IBA versus the temperature-adjusted solids loading.

(2) Krieger–Dougherty Model

The relationship between the viscosity and the solids volume percentage in a suspension has been modeled by Krieger and Dougherty[6] as

$$\eta = \eta_0\left(1 - \frac{\beta\phi}{\phi_0}\right)^{-[\eta]\phi_0} \tag{5}$$

In Eq. (5), η is the viscosity of the suspension and η_0 is the viscosity of the solvent. The variable ϕ_0 is the theoretical packing factor; a maximum packing fraction of 0.64 for random close packing is used in the following calculation. The true volume fraction of the powder dispersed in the suspension is represented by the variable ϕ. The intrinsic viscosity of the suspension (denoted as $[\eta]$) is a function of particle geometry; a value of $[\eta] = 2.5$ is appropriate for spherical particles. β is the effective packing factor of the ceramic powder; this factor is used to account for the thickness of the dispersant absorbed on the particles. No information on the thickness of the dispersant on our ceramic particles is available; therefore, this factor was determined empirically to be $\beta = 1.21$. Figure 9 shows that the model provided a satisfactory description to the solids-loading-corrected viscosity–solids-loading data for the Al_2O_3 suspension.

The β factor can be estimated from the ratio between the volume of the ceramic particles with and without the absorbed dispersant layer in the following expression:

$$\beta = \left(\frac{d + 2b}{d}\right)^3 \tag{6}$$

where d is the diameter of the particle and b is the adsorbed layer thickness. Using Eq. (6) and the value $\beta = 1.21$ from the empirical fit, the thickness of the absorbed layer of the dispersant on the spherical Al_2O_3 particle was estimated to be ~13 nm. This value is on the same order of the thickness of the adsorbed layer that was estimated by Bergström in his 50 vol% nonaqueous suspension.[16] The result suggests that the empirical β factor is in a reasonable range.

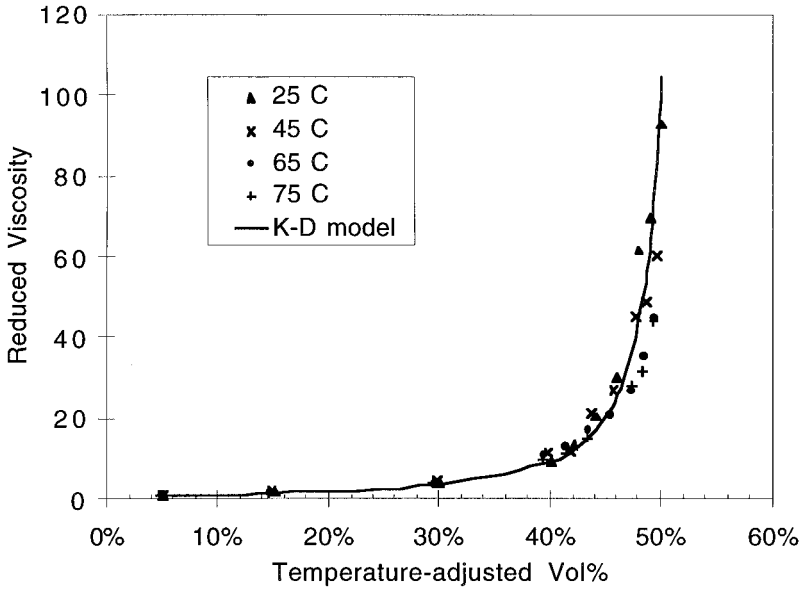

Fig. 9. Krieger–Dougherty model fitted to the experimental data of Al_2O_3/PNPGDA/IBA.

In the HA suspension, the ceramic powder is acicular, with an aspect ratio of 10. The intrinsic viscosity of the suspension is a function of the particle geometry; therefore, a modified intrinsic viscosity in the Krieger–Dougherty equation is needed to accommodate for the acicular nature of the powder. The HA suspension is not in the Brownian range; therefore, the theoretical intrinsic viscosity for Brownian rods[15] does not apply. For the non-Brownian cases, Barnes[4] proposed an equation for the intrinsic viscosity [η] of rod-shaped powders:

$$[\eta] = \frac{7 \times \left(\frac{L}{d}\right)^{5/3}}{100} \tag{7}$$

Thus, a value of [η] = 3.25 was appropriate. The Krieger–Dougherty model again was fitted to the viscosity data of the HA suspensions. The factor β = 1.58 was determined via empirical fitting. Figure 10 shows the match between the calculated and the experimental values; note that this observation explains the sharp increase in viscosity versus solids loading for the HA powder. The β factor again can be estimated from the ratio between the volume of the HA rods with and without the absorbed dispersant layer in the following expression:

$$\beta = \left(\frac{d + 2b}{d}\right)^2 \times \left(\frac{L + 2b}{L}\right) \tag{8}$$

where d is the diameter of the particle, L the length of the particle, and b the thickness of the adsorbed layer. Using Eq. (8), we determined that the factor β = 1.58 corresponded to an adsorbed-layer thickness of 6–8 nm on the powder, which is in the same thickness range that was calculated in our Al_2O_3 suspension. The parameters used in the Krieger–Dougherty model for both suspensions are listed in Table I.

The above-discussed results show that the viscosity data can be reconciled with the hydrodynamic Krieger–Dougherty theory, which suggests that the interparticle interactions are predominantly hydrodynamic. Floclike interactions are not necessary to reconcile the observation, which suggests that these suspensions are fully dispersed. The Krieger–Dougherty model is useful in providing the

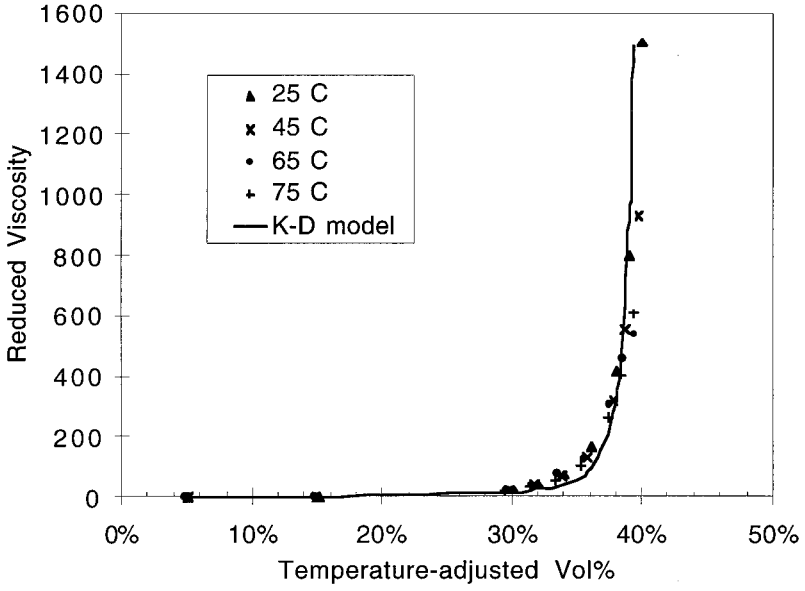

Fig. 10. Krieger–Dougherty model fitted to the experimental data of HA/PNPGDA/IBA.

Table I. Parameters Used in Krieger–Dougherty Models

Model	Effective packing factor, β	Intrinsic viscosity, η	Maximum packing, ϕ_0
HA/PNPGDA/IBA	1.58	3.25	0.64
Al_2O_3/PNPGDA/IBA	1.21	2.50	0.64

mathematics in regard to the effect of solids loading on the suspension viscosity. The model is useful, even with these considerably complicated suspension systems that include ceramic powders, nonaqueous acrylate liquid medium, and commercial dispersants. The model describes spherical particle suspensions well. With the modified intrinsic viscosity, the same model also can describe the acicular-HA-particle-filled suspension.

In practice, the model curves obtained with the Krieger–Dougherty equation can be used as the master curves to estimate the high-shear Newtonian viscosity of our suspensions at various temperatures. A master curve will be needed only for the temperature range of interest. For a suspension of a given solids loading at room temperature, the effective solids loading at the processing temperature can be calculated first. The corresponding reduced viscosity can be estimated from the model, and the apparent viscosity of the suspension at that temperature can be obtained.

IV. Conclusions

The effect of temperature and solids loading on the viscosity of a nonaqueous Al_2O_3 suspension and a HA suspension was studied. The solids-loading–viscosity curves for both suspensions were reduced by the temperature-adjusted solids loading and the reduced viscosity. The results show that these two variables are the dominant factors in controlling the high-shear Newtonian viscosity of the suspension at various temperatures.

The Krieger–Dougherty model has provided a satisfactory description of our reduced solids-loading–viscosity data of both suspensions. The results suggest that the particles in the suspensions are fully dispersed and that a hydrodynamic Krieger–Dougherty theory is needed only to reconcile the data.

Acknowledgments

The authors would like to acknowledge Susan Lee (Sanders Design International, Inc., Wilton, NH) for her assistance in measuring the coefficient of thermal expansion of the monomer premix. The authors also would like to thank Prof. M. J. Solomon (Dept. of Chemical Engineering, University of Michigan) for his helpful suggestions and discussions.

References

[1]T.-M. G. Chu, "Solid Freeform Fabrication of Biomaterials"; Ph.D. Thesis. University of Michigan, Ann Arbor, MI, 1999.

[2]K. Seerden, N. Reis, B. Derby, P. Grant, J. Halloran, and J. Evans, "Direct Ink-Jet Deposition of Ceramic Green Bodies: I—Formulation of Build Materials"; pp. 141–46 in Materials Research Society Symposium Proceedings, Vol. 542, *Solid Freeform and Additive Fabrication* (Boston, MA, 1998). Edited by D. Dimos, S. C. Danforth, and M. J. Cima. Materials Research Society, Pittsburgh, PA, 1998.

[3]N. Reis, K. Seerden, B. Derby, J. Halloran, and J. Evans, "Direct Ink-Jet Deposition of Ceramic Green Bodies: II—Jet Behavior and Deposit Formation"; *ibid*, pp. 147–52.

[4]H. Barnes, J. Hutton, and K. Walters, "Rheology of Suspensions"; pp. 115–39 in *An Introduction to Rheology*. Edited by H. Barnes. Elsevier, New York, 1989.

[5]A. I. Jomha, A. Merrington, L. V. Woodcock, H. A. Barnes, and A. Lips, "Recent Developments in Dense Suspension Rheology," *Powder Technol.*, **65**, 343–70 (1991).

[6]I. M. Krieger and T. J. Dougherty, "A Mechanism for Non-Newtonian Flow in Suspensions of Rigid Spheres," *Trans. Soc. Rheol.*, **3**, 137–52 (1959).

[7]R. Sudduth, "A Generalized Model to Predict the Viscosity of Solutions with Suspended Particles, I," *J. Appl. Polym. Sci.*, **48**, 25–36 (1993).

[8]J. van der Werff and C. de Kruif, "Hard-Sphere Colloidal Dispersions: The Scaling of Rheological Properties with Particle Size, Volume Fraction, and Shear Rate," *J. Rheol. (NY)*, **33**, 421–54 (1989).

[9]I. M. Krieger, "A Dimensional Approach to Colloid Rheology," *Trans. Soc. Rheol.*, **7**, 101–109 (1963).

[10]A. Tsutsumi and K. Yoshida, "Effect of Temperature on Rheological Properties of Suspensions," *J. Non-Newtonian Fluid Mech.*, **26**, 175–83 (1987).

[11]D. C. Le and S. N. Bhattacharya, "Influence of Temperature on the Viscous Behavior of Some Concentrated Dispersions," *J. Rheol. (NY)*, **34**, 637–55 (1990).

[12]Y. Papir and I. Krieger, "Rheological Studies on Dispersions of Uniform Colloidal Spheres, II. Dispersions in Nonaqueous Media," *J. Colloid Interface Sci.*, **34**, 126–30 (1970).

[13]A. Ruys, M. Wei, C. Sorrell, M. Dickson, A. Brandwood, and B. Milthorpe, "Sintering Effects on the Strength of Hydroxyapatite," *Biomaterials*, **16**, 409–15 (1995).

[14]T. M. Chu, J. W. Halloran, S. J. Hollister, and S. E. Feinberg, "Hydroxyapatite Implants with Designed Internal Architecture," *J. Mater. Sci.: Mater. Med.*, in press.

[15]R. G. Larson, "Particulate Suspensions"; pp. 263–323 in *The Structure and Rheology of Complex Fluids*. Edited by R. G. Larson. Oxford University Press, New York, 1999.

[16]L. Bergström, "Rheological Properties of Concentrated, Nonaqueous Silicon Nitride Suspension," *J. Am. Ceram. Soc.*, **79** [10] 3033–40 (1996). □